J Therm Anal Calorim (2012) 109:1277–1284
DOI 10.1007/s10973-012-2568-z

TMDSC phase angle for a better nanocomposite interphase identification

Javier Tarrío-Saavedra · Carlos Gracia-Fernández · Jorge López-Beceiro · Salvador Naya · Ramón Artiaga

NATAS2011 Conference Special Chapter

Abstract The present study suggests a new approach, based on the utilization of temperature modulated differential scanning calorimetry (TMDSC) technique, for identifying and characterizing the organic–inorganic interphase of two materials: an epoxy–fumed silica nanocomposite and a thermoplastic polyurethane (TPU)–multiwalled nanotube (MWNT) composite. The approach used here makes use of TMDSC data and basically consists of using the phase angle or the derivative of the reversing heat flow instead of the reversing heat flow curve itself. In the case of epoxy–fumed silica composites, two glass transition regions were identified. The glass transition temperature (T_g) of the composite was observed to vary as a consequence of the filler content. This study shows that the T_g variation is due to the formation of an organic–inorganic interphase, with its own glass transition temperature, which is different from the epoxy matrix T_g. In the case of TPU–MWNT composites, two relaxations and an additional first order transition were observed: the first relaxation corresponds to the hard segment, the second is related to an interaction between filler and matrix and the third process may be connected to the partial melting of the hard segment. The addition of 0.5 wt% MWNT causes a small reduction in T_g of the TPU. A major nanotube addition, 10 wt%, induces the appearance of a new relaxation that may be associated with the existence of an interface. In general, a better separation between the matrix and interphase glass transitions was obtained by the TMDSC phase angle signal.

Keywords Nanocomposites interphase · TMDSC · Phase angle · Nanotubes · Fumed silica

J. Tarrío-Saavedra (✉) · J. López-Beceiro · S. Naya · R. Artiaga
Higher Polytechnic School, University of A Coruña, Campus de Esteiro, 15403 Ferrol, Spain
e-mail: jtarrio@udc.es

C. Gracia-Fernández
Thermal Analysis, Rheology and Microcalorimetry Applications, TA Instruments-Waters Cromatografía, S.A. Avda. Europa, 21 Parque Empresarial La Moraleja, 28108 Alcobendas, Madrid, Spain

Introduction

Today, the intense development of new nanocomposites, consisting of a polymer matrix and an inorganic phase, transforms the study and characterization of the organic–inorganic interphase in an increasingly recurrent theme in polymer science. This study is justified from the perspective that the proper characterization of the interphase produced in a nanocomposite is crucial to understanding the properties and behavior of the final material. Despite their importance, its identification, characterization and subsequent relationship with the final properties of the material presents serious difficulties depending on the case. For this reason, in the present study, a new approach based on the utilization of temperature modulated differential scanning calorimetry (TMDSC) technique, is suggested for identifying and characterizing the organic–inorganic interphase produced in nanomaterials such as fumed silica-filled epoxy and thermoplastic polyurethane (TPU)–multiwalled nanotube (MWNT) composites.

The degree of interaction between filler and polymer and thus the composite properties have been related to the filler-matrix interphase. In fact, synergistic effects were found in the form of a further increase in wear resistance, stiffness, fracture toughness and tensile and impact strengths by

adding nano and microparticles [1–3]. As defined by Drzal et al. [4], and Schadler [5], the interfacial region is the region beginning at the point in the fiber at which the properties differ from those of the bulk filler and ending at the point in the matrix at which the properties become equal to those of the bulk matrix. In fact, the interphase is different from the matrix both in relation to the degree of cure as well as in the actual chemical structure. Even, the mobility of polymer chains is different. Therefore, the T_g of the interphase (assuming it exists) may be different from the matrix [5]. The thickness of the interphase is usually between 2 and 50 nm [5] and has a very significant impact on the properties of the nanocomposite. Thus, if the T_g of the interphase is less than the T_g of the polymer matrix, the final T_g of the resulting nanocomposite tends to decrease with the addition of filler. Alternatively, if the T_g of the interphase is greater than the T_g of the matrix, the T_g of the nanocomposite tends to increase with filler content [6]. However, this trend may not hold for the entire range of filler content, since there are other factors such as the agglomeration effect [7]. In short, the change in the properties of a nanocomposite with the addition of nanofiller gives information about the existence of an organic–inorganic interphase and, if available, the direction and magnitude of this variation can characterize this interphase. But, is TMDSC an adequate technique to measure that subtle change of properties? This paper introduces a new means to extract the maximum information from TMDSC experiments.

Thermal analysis techniques are routinely applied in the study of thermal stability [8, 9], curing [6, 9], glass transition [1, 6, 10, 11] and thermomechanical properties corresponding to polymers and composites [12, 13]. In fact, in the present work, TMDSC is used to study the glass transition regions corresponding to matrix and interphase. Thus, we study the dynamic glass transition, which is used to describe the increasing relaxation time in the stable or metastable equilibrium state [14] and it is usually determined in heating by TMDSC. TMDSC is a refinement of standard DSC allowing for separation of overlapping reversing and non-reversing heat transfer events, such as the glass transition and enthalpy recovery [6, 10, 11]. Thus, TMDSC is able to measure simultaneously the total or underlying heat flow (HF) and the reversing signal, HF_{rev}, corresponding to the heat flow due to the heat capacity, which usually changes in an orderly fashion with temperature. When TMDSC is used, a sinusoidal oscillation is superimposed on a conventional linear cooling or heating ramp. This can be explained through the following expression:

$$T = T_0 + \beta \cdot t + A_T \cdot \sin(w \cdot t)$$

where T_0 is the initial temperature of the experiment, A_T the temperature modulation amplitude, β the heating rate, t the time and w the sinusoidal function frequency.

The reversing heat capacity, $C_{p_{rev}}$, is defined as

$$C_{p_{rev}} = K_{C_p} \cdot \frac{A_{HF}}{A_T \cdot w}$$

where K_{C_p}, A_T and $A_T \cdot w$ are the calibration constant, temperature amplitude, and heating rate amplitude, respectively. The heat flow reversing component (HF_{rev}), is equal to $C_{p_{rev}}$ multiplied by the underlying heating rate. Moreover, the non-reversing or time-dependent heat flow ($HF_{non\text{-}rev}$) can be obtained from HF_{rev} and HF using the expression

$$HF = HF_{rev} + HF_{non\text{-}rev} \Rightarrow \frac{dH}{dt} = C_{p_{rev}} \cdot \frac{dT}{dt} + f(t, T).$$

Another useful component is the phase angle, which arises from the modulation shift between the modulated and detected temperature. It is the phase shift between the input and response [15]: the stimulus is the modulated heating rate and the response is the modulated heat flow. This signal is especially suited to observe relaxation phenomena during cure [15, 16] showing more sensitivity and resolution than other signals like HF_{rev} [15]. In TMDSC, the dynamic glass transition temperature, T_{gd}, is affected by the temperature modulation frequency (as the DMA T_{gd} is affected by the mechanical frequency) and it is generally measured using the reversing heat flow. Nevertheless, as was mentioned, the TMDSC phase can be also used to measure relaxations. In fact, an increase of the phase angle occurs at the glass transition region. Therefore, it is possible to measure the glass transition temperature from the maximum of the phase angle peak [17].

The advantages of TMDSC with respect to standard DSC can be summarized with the following points: MTDSC allows calculation of the heat capacity in a single measurement (in both the quasi-isothermal mode and dynamic mode, which basically consist in applying a modulation on the average heating rate, even in the quasi-isothermal case of zero heating rate), it allows simultaneous measurement of the reversing and non-reversing heat flow, the heat capacity sensitivity is increased thanks to the relatively high modulated heating rate and it allows ramp tests using very low average heating rates, improving the resolution and sensitivity, the separation of complex transitions and obtaining more precise measurements of the degree of crystallinity. Another important difference is that T_g measured by TMDSC is higher than T_g from standard DSC. This is due to the effect of frequency: the higher the modulation frequency, the higher the observed glass transition temperature [11, 15]. This is also the reason for the differences between T_g obtained by 1 Hz DMA and TMDSC: T_g measured by DMA is higher because a higher test frequency is used [17]. This article shows how different

relaxations can be observed through different TMDSC signals. The two nanomaterials studied are an epoxy–fumed silica composite and a TPU–MWNT composite.

Briefly, TPUs are linear block copolymers that are composed of two types of segments: hard segment with high T_g (diisocyanate and, generally, diol or diamine) and soft segment with low T_g (consisting of a linear and long chain diol such as polyether and polyester diol). The hard segments, composed of polar materials, can form carbonyl to amino hydrogen bonds and thus tend to cluster or aggregate into ordered hard domains, whereas the soft segments form amorphous domains. Thus, the hard segment structure is semicrystalline, while the soft one presents a rubbery structure and T_g below room temperature. T_g can be studied by standard DSC [18, 19] but in the case of the hard segment phase, the glass transition can be not detected due to the small change in heat capacity. In fact, many studies recommend dynamic mechanical analysis (DMA) instead of DSC [20, 21]. However, it seems that the use of TMDSC has not been sufficiently exploited in the study of the hard segment relaxation. Apart from this, the introduction of inorganic fillers into the TPU matrix can improve the mechanical properties of the material and the thermal stability, both in a chemical sense and mechanically, increasing the upper use temperature. Many studies rely on that approach [18, 22–25]. Of particular interest is the case of nanotube addition due to their high mechanical strength, thermal and electrical conductivity, aspect ratio, and thermal stability. The addition of MWNT to a TPU matrix can produce improvements in all these properties [22–25].

On the other hand, the formation of epoxy–fumed silica nanocomposites can provide dimensional stability, glass transition modification, flame retardance, thermal stability, variable dielectric constant or gas barrier and corrosion protection [7, 8, 26–30].

A good dispersion of the filler agglomerates promotes an increase of the organic–inorganic interfacial surface and thus, is necessary for obtaining improvements in the properties mentioned. The aim of this study is to provide new insight into identification of the interfacial regions, whose relaxation times are different from those of the matrix, by TMDSC.

Experimental

A two component epoxy system consisted of a diglycidyl ether of trimethylolpropane-based resin, Triepox GA, from Gairesa (Valdoviño, Spain) and the curing agent 1,3-benzenedimethanamine 99 % pure, is used [31, 32]. The fumed silica (provided by Ferroatlántica I + D, Spain) is a by-product derived from the silicon production in electrical melting furnaces by the reduction of high purity quartz at 1,800 °C. It is a fine powder consisting of amorphous SiO_2 of variable purity, with a mean particle size of 0.15 μm (it is a mixture of nano and micro particles) measured by the SediGraph method with a surface area equal to 20 $m^2\ g^{-1}$.

Composite samples for TMDSC tests were obtained for 0, 5, 10, 20, 30, 40, and 50 wt% of fumed silica content where hardener and epoxy resin were mixed in stoichiometric proportions, stirred for 15 min and sonicated for another 5 min (to obtain, as far as possible, a uniform distribution), cured at room temperature for 24 h and post-cured at 90 °C for 2 h. According to manufacturer recommendations and previous trial experiments, this treatment would ensure a fully cure of the system. It was then verified by observation of no residual cure in the DSC tests and by the fact that the same T_g is observed in repeated scans of the same sample. For the case of epoxy–fumed silica composites, the TMDSC experiments were performed on a TA Instruments MDSC Q-2000 attached to a mechanical cooling system. The following calibrations were performed, according to manufacturer recommended procedures: Tzero, enthalpy constant, temperature, and modulated heat capacity. The DSC was operated in modulated mode in order to separate the reversing from non-reversing phenomena such as enthalpic recovery, residual cure, and possible degradation processes taking place in cured samples. The thermal program consisted of a 5 °C min^{-1} average heating ramp from −20 to 200 °C. The modulation amplitude was 1.6 °C and the period 60 s. The experiments corresponding to TPU–MWNT nanocomposites were performed on a TA Instruments MDSC Q-20. The temperature range was between 40 and 100 °C. The modulation amplitude was 0.48 °C and the period 60 s.

For the case of TPU–MWNT nanocomposites, the matrix is a TPU consisting of 50 % by mass hard segment and 50 % soft segment. Multi walled nanotubes (MWNT) consisting of multiple rolled layers (concentric tubes) of graphite were provided by Helix Material Solutions, Inc. Richardson TX, USA. Purity is about 95 % according to manufacturer specifications (their length is between 0.5 and 40 μm and the specific surface area is in the range from 40 to 300 $m^2\ g^{-1}$). The thermal program consisted of a 3 °C min^{-1} average heating ramp from 40 to 130 °C. The modulation amplitude was 0.48 °C and the period 60 s. These parameter values were chosen in order to have 5 cycles at least along the transition under study, and also to have heat only conditions (non negative heating rate at any moment), which would prevent intercalated melting-crystallization processes of TPU.

Results

As mentioned earlier, the main objective of this study is to evaluate the possibilities for thermal analysis, in particular for TMDSC, as a valid and useful method to conveniently

identify and characterize the interphase produced within a nanocomposite. Thus, two different materials were tested for this purpose: epoxy–fumed silica and TPU–MWNT nanocomposites.

Epoxy–fumed silica nanocomposites

Of the existing qualitative techniques to identify phases in nanomaterials, transmission electron microscopy (TEM) stands out because it is also used to measure the degree of dispersion of nanoparticles within the matrix [33, 34]. Thus, Fig. 1 corresponds to a TEM micrograph obtained from a nanocomposite with 10 wt% silica. TEM micrographs did not clearly reveal the existence or absence of an interphase (there is no significant color intensity differences around the nanoparticles). The interphase is too thin or the opacity to electrons is similar to that of the matrix. Nevertheless, the picture suggests the existence of air traps. We could have concluded that there is no interaction between the polymer and particles of fumed silica, however, the use of other techniques such as DMA are also employed for this purpose and can give more information. In fact, DMA tests of the same material indicated the existence of an interphase [7]. According to Reed [35], the existence of a shoulder on phase angle tangent (tan δ) can be attributed to the particle-resin interphase.

Both in DMA and TMDSC, the T_{gd} can be measured using the phase angle signal (instead of using the HF_{rev} in TMDSC and tan δ in DMA) between the stimulus and the response. In DMA, the stimulus is a sinusoidal strain oscillation and the response is a sinusoidal stress oscillation. In the same way, in TMDSC, the stimulus is the modulated heating rate and the response is the modulated heat flow [15]. The commonality of the DSC and DMA signals, measured at the same frequency and isothermal conditions, has been proved [17]. As an increase of the phase angle signal is produced at the glass transition region, giving a well defined peak, this criterion is valid to study the glass transition relaxation phenomena [17].

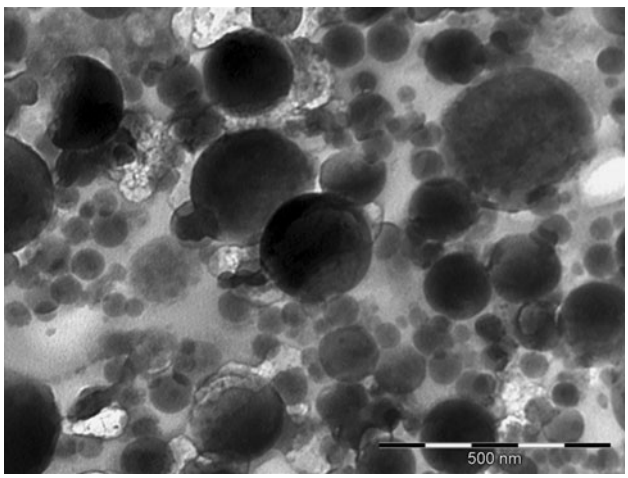

Fig. 1 TEM micrograph corresponding to a 10 wt% silica content nanocomposite

Therefore, the use of the phase angle obtained by TMDSC provides information about the same relaxation process or processes as DMA. So, while the DSC technique measures the change in C_p at the glass transitions, the TMDSC and DMA measure the relaxation associated with the glass transition. This relaxation can be more easily detected than the C_p change when the amorphous fraction is relatively small, as it happens in crystalline polymers, what makes TMDSC more useful in this case (in addition to separating the effects of enthalpy relaxation or crystallization). We use the phase angle because it is more sensitive than other signals, as in other techniques such as DMA. Figure 2 shows the δ curves obtained from the unfilled sample and composites with different filler contents using the TMDSC experimental conditions described in Experimental section. It can be observed that there is only one transition in the case of the neat epoxy sample. Nevertheless, two different relaxations are observed when silica is added. In this particular study, using TMDSC, at the experimental conditions described, provides δ curves where the two relaxation processes are observed. The T_{gd} of the non-filled sample is clearly observed at about 80 °C. Addition of filler at any rate produces a double T_g. Thus, one of them would correspond to the matrix and the other to the interface between the resin and the silica. In principle, the higher temperature peak can be assigned to the interface since the polymer chains mobility would be restricted by the polymer–silica bonds. Nevertheless, an important decrease of both relaxations with respect to the non-filled sample T_g is also observed. This effect was attributed to agglomerates formation and air trapping during the preparation of the composites with low filler contents [7] and matches with the presence of air traps observed in Fig. 1. On the other hand, an increase of both T_{gd} is observed when increasing the filler content above the 30 wt%. This increasing trend was associated to agglomerates destruction because, due to their higher viscosity, important shear stresses are generated while stirring the resin-filler mixture [7]. Using the phase angle signal supports the existence of a second relaxation process attributable to the presence of matrix-reinforcement interface. Thus, the existence of a second relaxation process is detected by TMDSC.

Moreover, these curves can be compared to other signals obtained by TMDSC. The more usual way to study the glass transition by TMDSC is through the observation of HF_{rev} curves. Figure 3 shows the traces obtained from composites with different filler contents using the same

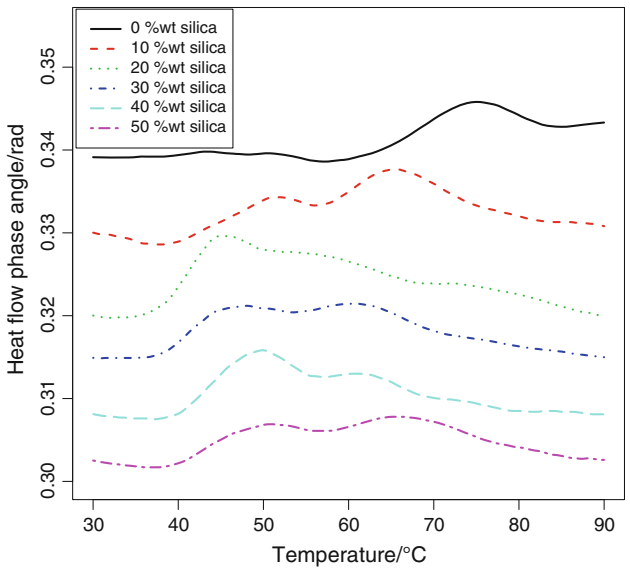

Fig. 2 Phase angle (δ) curves obtained from composites with different filler contents using modulation amplitude of 1.6 °C and a period corresponding to 60 s. Two different relaxations are clearly observed when silica is added

modulation parameters. Two different relaxations are observed, but not as well separated as in the δ curves.

In order to obtain more sensitivity and resolution, the HF_{rev} derivatives with respect to temperature are calculated. A drawback of this procedure is that the resulting derivatives may contain significant noise when calculated by numerical methods. To avoid this, the derivatives are calculated from the nonparametric local linear estimator used to fit the experimental HF_{rev}. A direct plug-in bandwidth selection method [36] was used to select the smoothing parameter. The results are shown in Fig. 4. A significant reduction of noise is observed without sacrificing information contained in the curve. The traces present many similarities with the δ curves (except peaks are in the opposite direction): two defined relaxation peaks are observed with a similar area ratio, for each sample. These derivatives present a better resolution than δ curves in the 20 and 30 wt% cases, while δ curves present a better resolution for the 50 wt% sample. The use of these two types of curves gives complementary information about the two relaxation processes. And the derivative of HF_{rev} provides a much better resolution than the HF_{rev} curves.

TPU–MWNT nanocomposites

Figure 5 shows the total heat flow curves obtained from TPU–MWNT composites with different filler contents using the TMDSC experimental conditions described in Sect. 2. The baseline has been subtracted from the different DSC curves. For the case of 0 wt% MWNT, there appears to be two different transitions, represented by two peaks at about 60 and 80 °C, but the signal does not have sufficient resolution to be definitive. When nanotubes are added, the signals become more complicated and it is difficult to distinguish between relaxation processes and other possible phenomena like enthalpic relaxations. Even so, several studies report the existence of a glass transition region corresponding to the hard segment measured by DSC [18, 19, 37]. Koberstein et al. [18] proposed that the DSC transitions in the 50–90 °C temperature range are due to an apparent hard microdomain glass transition process. In

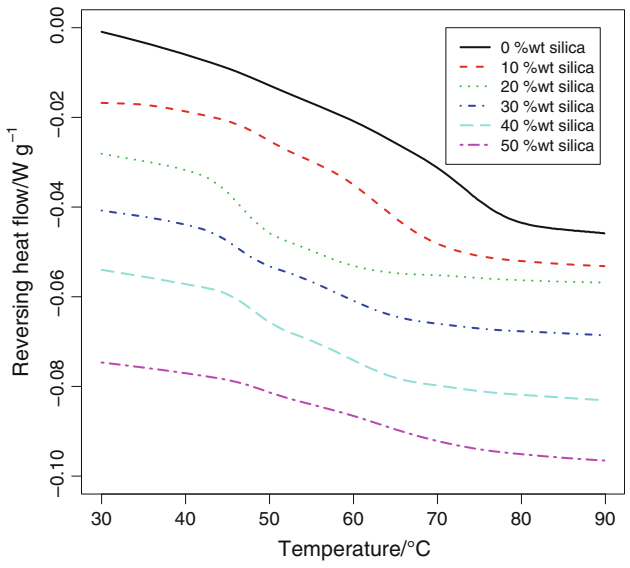

Fig. 3 HF_{rev} curves obtained from composites with different filler contents using modulation amplitude of 1.6 °C and a period corresponding to 60 s

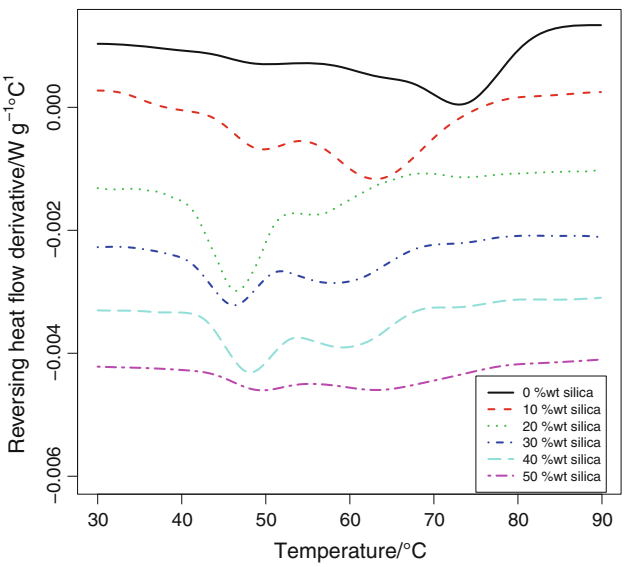

Fig. 4 HF_{rev} derivatives obtained using a nonparametric local linear model

addition, Chen et al. studied the nature of the DSC peak that is reported in the literature as the T_1 peak. They concluded that T_1 endotherm is the enthalpy relaxation behavior resulting from a prolonged physical aging process, related to the glass transition. Therefore the first step of the three curves in Fig. 5 could be connected to the hard segment glass transition and the associated endothermic peak (in 0.5 wt% curve) may be related to T_1. A second endotherm, referred as T_2, was observed in TPU at about 100 °C [19, 37]. In the present work, that second endotherm appears at about 80 °C. In this context, reversing C_p and δ signals would provide a good insight for better understanding of the nature of this transition.

To discern the relaxations from other phenomena it is necessary to use additional TMDSC signals such as HF_{rev} and reversing C_p $\left(C_{p_{rev}}\right)$. In fact, the more usual way to study the glass transition by TMDSC is through observation of these curves. Figure 6 shows the $C_{p_{rev}}$ traces obtained from composites with different MWNT contents. At least one relaxation can be observed in all the traces, but there is too much noise in the case of 0 wt% sample and there is little signal sensitivity in 0.5 wt% and 10 wt% traces. For obtaining more sensitivity and resolution, calculating the $C_{p_{rev}}$ derivatives with respect to temperature could be useful. As in the epoxy–fumed silica case, the only drawback of this procedure is that the resulting derivatives may contain significant noise when calculated by numerical methods. That is why the aforementioned nonparametric local linear estimator is used to fit the experimental $C_{p_{rev}}$, from which we calculate the first derivative. The estimator optimal bandwidth (smoothing parameter) is obtained by a plug-in method again [36]. But a considerable amount of noise is still observable and it is hard to identify single peaks and their related relaxations or first order transitions. Thus, these curves are not included in the present work.

Finally, δ curves are plotted in Fig. 7. One relaxation is observed in the 0 wt% trace above 60 °C. It is important to note that this is related to the glass transition of the polyurethane hard segment [18, 19, 37]. The other transition that takes place above 80 °C is a first order transition [38] and it may be related to the melting of crystalline hard segment [18, 19, 37]. Thus, the TMDSC δ signal improves the sensitivity relative to the standard DSC measurement. Each relaxation or first order transition is connected to one peak on the δ curve. In Table 1, the hard segment T_g values (T_{g1}) and T_2 (related to the relaxation at above 80 °C) are defined as the temperature corresponding to the maximum of each δ curve peak.

A decrease of the T_{g1} is observed when 0.5 wt% MWNT is added. The hard segment relaxation is displaced to lower temperatures (T_{g1} decreases). Nevertheless, when 10 wt% MWNT is added, the hard segment relaxation is moved to higher temperatures. Considering that in these systems percolation occurs at about 2–5 % [39], at 0.5 % the system is well below the percolation concentration. In these conditions the nanotubes may interfere with the polymer chains increasing the distance between macromolecule

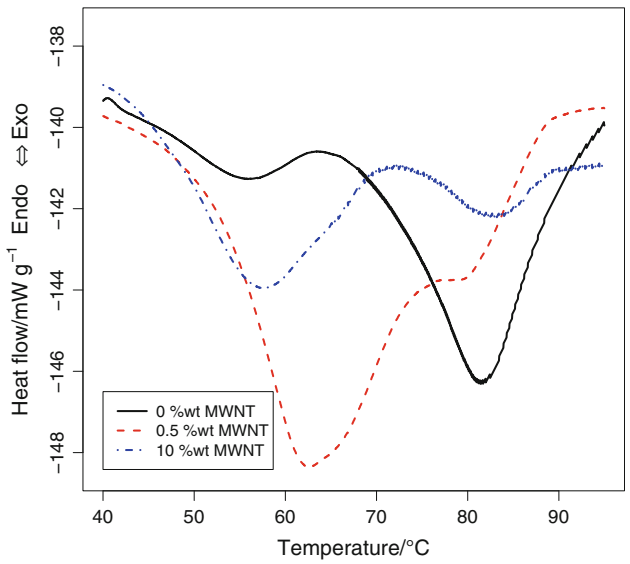

Fig. 5 Total heat flow curves obtained from composites with different MWNT contents using modulation amplitude of 0.48 °C and a period corresponding to 60 s

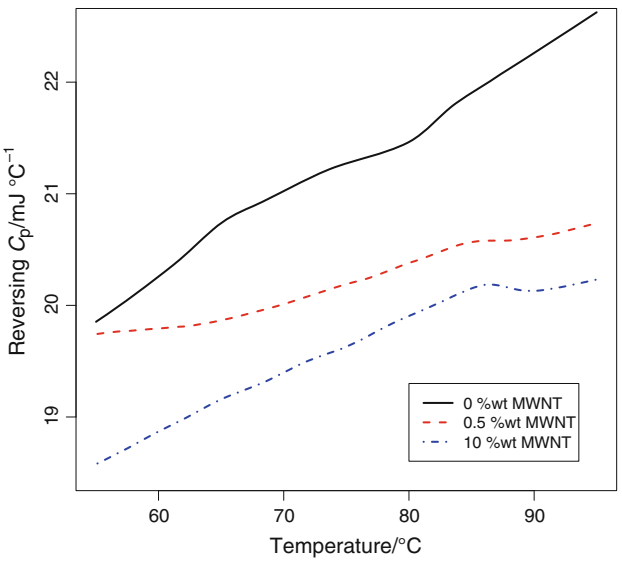

Fig. 6 $C_{p_{rev}}$ curves obtained from composites with different filler contents using modulation amplitude of 0.48 °C and a period corresponding to 60 s

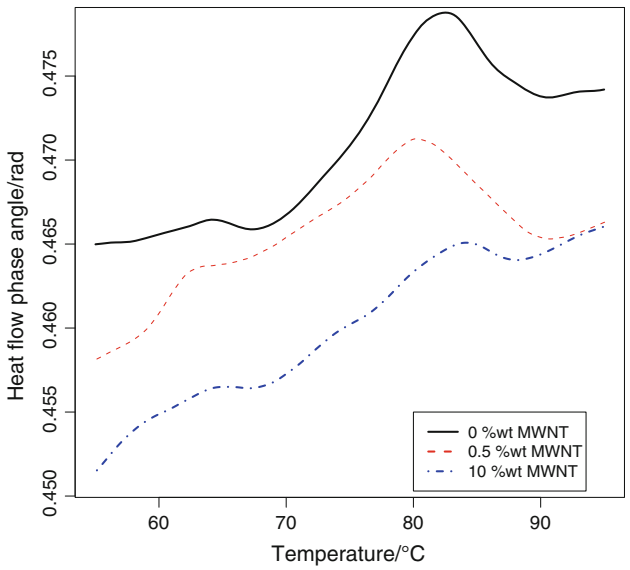

Fig. 7 Phase angle (δ) curves obtained from composites with different filler contents using modulation amplitude of 0.48 °C and a period corresponding to 60 s

Table 1 Glass transition temperatures corresponding to each relaxation and first order transition

MWNT content/wt%	T_{g1}/°C	$T_{gInterface}$/°C	T_2/°C
0	64.25	–	82.60
0.5	62.50	–	80.24
10	65.50	73.50	84.14

segments and thus, increasing the free volume. On the other hand, 10 % is above the percolation limit and in these conditions the nanotubes are expected to increase the stiffness of the system. There is also a new additional slight relaxation between the two main ones (at 73.5 °C, see Fig. 7). One may think that it is too weak and could be attributed to experimental error. Nevertheless, it was confirmed by repeating the experiments and was observed to increase with the nanotubes content. This relaxation was observed by DMA as reported in other works [40]. Thus, this new relaxation may be related to the interfacial region produced by the organic–inorganic interaction. In fact, it is better observed on the highest filler content sample (10 %), which is an indication that the size of the relaxation is associated to the interfacial area. Nevertheless, only the δ signal is able to provide the proper sensitivity and resolution to distinguish such new relaxations.

Conclusions

The possibilities of thermal analysis, in particular of the TMDSC, have been evaluated for conveniently identifying the existence of an additional relaxation corresponding to the formation of an organic–inorganic interphase in epoxy–fumed silica and in TPU–MWNT nanocomposites.

TMDSC phase angle signal is used in the present study, for the first time, for the identification of the nanocomposite interface.

Focusing on epoxy–fumed silica composites, TMDSC curves show that the T_g variation is due to the formation of an organic–inorganic interphase, with its own glass transition temperature, which is different from that of the epoxy matrix and is related to the organic–inorganic nanocomposite interphase. Moreover, the use of the HF_{rev} derivative provides a much better resolution than the HF_{rev} curves to identify the second relaxation related to the interphase.

In the case of TPU–MWNT nanocomposites, two different transitions were identified in the neat TPU using TMDSC phase angle. The first is related to the relaxation due to the glass transition of the hard segment and the second corresponds to a first order transition that may be connected to the partial crystallization of the amorphous hard segment. The ability to measure the glass transition of the hard segment using the TMDSC δ signal has been demonstrated. This signal provides more sensitivity and resolution than standard DSC.

The δ signal shows that the addition of 0.5 wt% MWNT results in a small decrease in the TPU T_g. This is attributed to an increase of the free volume originated by the CNT below the percolation concentration. However, a major addition of 10 wt% of nanotubes raises the hard segment glass transition to higher temperatures. Moreover, it also induces the appearance of a new relaxation that may be associated with the existence of an interface.

The phase angle signal was found to be more convenient and informative in characterizing the existing relaxations than $C_{p_{rev}}$ and HF_{rev}, the signals traditionally used to study the glass transition region.

Acknowledgements This research has been partially supported by the Spanish Ministry of Science and Innovation, Grant MTM2008-00166 (ERDF included) and Grant MTM2011-22393. The authors thank Senén Paz for constructive comments and the referees for their valuable suggestions.

References

1. Wetzel B, Haupert F, Zhang MQ. Epoxy nanocomposites with high mechanical and tribological performance. Compos Sci Technol. 2003;63:2055–206.
2. Park JH, Jana SC. The relationship between nano- and microstructures and mechanical properties in PMMA–epoxy–nanoclay composites. Polymer. 2003;44:2091–100.
3. Han J, Cho K. Nanoparticle-induced enhancement in fracture toughness of highly loaded epoxy composites over a wide temperature range. J Mater Sci. 2006;41:4239–45.

4. Drzal LT, Rich MJ, Koenig MF, Lloyd PF. Adhesion of graphite fibers to epoxy matrices. II. The effect of fiber finish. J Adhes. 1983;16:133–52.
5. Schadler LS. Polymer-based and polymer-filled nanocomposites. In: Ajayan PM, Schadler LS, Braun PV, editors. Nanocomposite science and technology. Weinheim: Wiley; 2003. pp. 77–135.
6. Prime RB. Thermosets. In: Turi E, editor. Thermal characterization of polymeric materials. 2nd ed. San Diego: Academic Press; 1997. pp. 1380–766.
7. Tarrío-Saavedra J, López-Beceiro J, Naya S, Gracia C, Artiaga R. Controversial effects of fumed silica on the curing and thermomechanical properties of epoxy composites. Express Polym Lett. 2010;4:382–95.
8. Tarrio-Saavedra J, López-Beceiro J, Naya S, Artiaga R. Effect of silica content on thermal stability of fumed silica/epoxy composites. Polym Degrad Stab. 2008;93:2133–7.
9. Huang GC, Lee JK. Isothermal cure characterization of fumed silica/epoxy nanocomposites: the glass transition temperature and conversion. Compos Part A Appl Sci Manuf. 2010;41:473–9.
10. Thomas LC. An introduction to the techniques of differential scanning calorimetry (DSC) and modulated DSC. In: Artiaga R, editor. Thermal analysis. Fundamentals and applications to material characterization. A Coruña: Publicaciones de la Universidade da Coruña; 2005. pp. 9–25.
11. Reading M, Hourston DJ. Modulated temperature differential scanning calorimetry: theoretical and practical applications in polymer characterisation. Dordrecht: Springer; 2006.
12. Artiaga R, García A. Fundamentals of DMA. In: Artiaga R, editor. Thermal analysis. Fundamentals and applications to material characterization. Coruña: Publicaciones de la Universidade da Coruña; 2005. pp. 183–206.
13. Chartoff RP, Menczel JD, Dillman SH. Dynamic mechanical analysis (DMA). In: Menczel JD, Prime RB, editors. Thermal analysis of polymers: fundamentals and applications. San Jose: Wiley; 2009. pp. 387–496.
14. Donth E. The glass transition. Relaxation dynamics in liquids and disordered materials. Berlin: Springer; 2001.
15. Menczel JD, Judovits L, Prime RB, Bair HE, Reading M, Swier S. Differential scanning calorimetry (DSC). In: Menczel JD, Prime RB, editors. Thermal analysis of polymers: fundamentals and applications'. New York: Wiley; 2009. pp. 7–239.
16. Van Assche G, Van Hemelrijck A, Rahier H, Van Mele B. Thermochim Acta. 1997;304(305):317.
17. Gracia-Fernández C, Gómez-Barreiro S, López-Beceiro J, Tarrío-Saavedra J, Naya S, Artiaga R. Comparative study of the glass transition temperature by DMA and TMDSC. Polym Test. 2010;29:1002–6.
18. Koberstein JT, Galambos AF, Leung LM. Compression-molded polyurethane block copolymers. 1. Microdomain morphology and thermomechanical properties. Macromolecules. 1992;25:6195–204.
19. Chen TK, Shieh TS, Chui JY. Studies on the first DSC endotherm of polyurethane hard segment based on 4,4′-diphenylmethane diisocyanate and 1,4-butanediol. Macromolecules. 1998;31:1312–20.
20. Tien YI, Wei KW. The effect of nano-sized silicate layers from montmorillonite on glass transition, dynamic mechanical, and thermal degradation properties of segmented polyurethane. J Appl Polym Sci. 2002;86:1741–8.
21. Chen TK, Chui JY, Shieh TS. Macromolecules. Glass transition behaviors of a polyurethane hard segment based on 4,4′-diisocyanatodiphenylmethane and 1,4-butanediol and the calculation of microdomain composition. Macromolecules. 1997;30:5068–74.
22. Xia H, Song M. Preparation and characterization of polyurethane–carbon nanotube composites. Soft Matter. 2005;1:386–94.
23. Xia H, Song M. Preparation and characterisation of polyurethane grafted single-walled carbon nanotubes and derived polyurethane nanocomposites. J Mater Chem. 2006;16:1843–51.
24. Koerner H, Price G, Pearce NA, Alexander M, Vaia RA. Remotely actuated polymer nanocomposites—stress-recovery of carbon-nanotube-filled thermoplastic elastomers. Nat Mater. 2004;3:115–20.
25. Cho JW, Kim JW, Jung YC, Goo NS. Electroactive shape-memory polyurethane composites incorporating carbon nanotubes. Macromol Rapid Commun. 2005;26:412–6.
26. Zhang H, Zhang Z, Friedrich K, Eger C. Property improvements of in situ epoxy nanocomposites with reduced interparticle distance at high nanosilica content. Acta Mater. 2006;54:1833–42.
27. Liu YL, Wei WL, Hsu KY, Ho WH. Thermal stability of epoxy–silica hybrid materials by thermogravimetric analysis. Thermochim Acta. 2004;412:139–47.
28. Preghenella M, Pegoretti A, Migliaresi C. Thermomechanical characterization of fumed silica–epoxy nanocomposites. Polymer. 2005;46:12065–72.
29. Yousefi A, Lafleur PG, Gauvin R. Kinetic studies of thermoset cure reactions: a review. Polym Compos. 1997;18:157–68.
30. Naya S, Martínez-Vilariño S, Artiaga R. Efecto de ciclos térmicos en la permeabilidad y propiedades térmicas de compuestos nanoarcilla-epoxi. Dyna's J. 2009;84:71–6.
31. Pellín MP, Regueira LN, Quintela AL, Losada PP, Gándara JS, Abuín SP. Epoxy resins based on trimethylolpropane. II. Kinetic and thermodynamic parameters of cure with m-XDA. J Appl Polym Sci. 1995;55:1507–16.
32. Quintela AL, Pellin MP, Abuin SP. Epoxidation reaction of trimethylolpropane with epichlorohydrin: kinetic study of chlorohydrin formation. Polym Eng Sci. 1996;36:568–73.
33. Jena PK, Brocchi EA, Solórzano IG, Motta MS. Identification of a third phase in Cu–Al_2O_3 nanocomposites prepared by chemical routes. Mater Sci Eng A Struct Mater Prop Microstruct Process. 2004;371:72–8.
34. Kim D, Lee JS, Barry CMF, Mead JL. Microscopic measurement of the degree of mixing for nanoparticles in polymer. Nanocomposites by TEM images. Microsc Res Tech. 2007;70:539–46.
35. Reed KE. Dynamic mechanical analysis of fiber reinforced composites. Polym Compos. 1980;1:44–9.
36. Ruppert D, Sheather SJ, Wand MP. An effective bandwidth selector for local least squares regression. J Am Stat Assoc. 1995;90:1257–70.
37. Finnigan B, Halley P, Jack K, McDowell A, Truss R, Casey P, Knott R, Martin D. Effect of the average soft-segment length on the morphology and properties of segmented polyurethane nanocomposites. J Appl Polym Sci. 2006;102:128–39.
38. Kultys A, Rogulska M, Pikus S, Skrzypiec K. The synthesis and characterization of new thermoplastic poly(carbonate-urethane) elastomers derived from HDI and aliphatic–aromatic chain extenders. Eur Polym J. 2009;45:2629–43.
39. Fernández M, Landa M, Muñoz ME, Santamaría A. Thermal and viscoelastic features of new nanocomposites based on a hot-melt adhesive polyurethane and multi-walled carbon nanotubes. Macromol Mater Eng. 2010;295:1031–41.
40. Fernández I, Santamaría A, Muñoz ME, Castell P. A rheological analysis of interactions in phenoxy/organoclay nanocomposites. Eur Polym J. 2007;43:3171–6.